Vastatin is an Endogenous Antiangiogenesis Polypeptide Lost in Hepatocellular Carcinoma and Effectively Inhibits Tumor Metastasis

Zan Shen[1], Chen Yao[2], Zifeng Wang[3], Lu Yue[4], Zheping Fang[5], Hong Yao[6], Feng Lin[1], Hui Zhao[1], Yuan-Jue Sun[1], Xiu-wu Bian[7], Xiaomei Wang[8], Yi Li[9], Gang Lu[9], Wai Sang Poon[9], Hsiang-Fu Kung[7] and Marie Chia-mi Lin[8]

This article has been corrected since Advance Online Publication and a erratum is also printed in this issue.

[1]*Department of Oncology, Affiliated 6th People's Hospital, Shanghai Jiaotong University, Shanghai, China;* [2]*Department of Orthopaedics, Affiliated 6th People's Hospital, Shanghai Jiaotong University, Shanghai, China;* [3]*Sun Yat-sen University Cancer Center, State Key Laboratory of Oncology in South China, Collaborative Innovation Center for Cancer Medicine, Guangzhou, China;* [4]*Department of Oncology, Affiliated Hospital of Medical College, Qingdao University, Qingdao, China;* [5]*Department of Hepatobiliary Surgery, Taizhou Hospital, Wenzhou Medical University, Zhejiang, China;* [6]*Jiangsu Engineering Laboratory of Cancer Biotherapy, Xuzhou Medical College, Xuzhou, China;* [7]*Institute of Pathology, Southwest Cancer Center, Chongqing, China;* [8]*Shenzhen Key Laboratory of Translational Medicine of Tumor, School of Medicine, Shenzhen University, Shenzhen, China;* [9]*Brain Tumor Centre, Department of Surgery, The Chinese University of Hong Kong, Hong Kong, China*

Hepatocellular carcinoma (HCC) is a hypervascular cancer without effective treatment. Here, we report that polypeptide of NC1 domain of type VIII collagen (vastatin) is an endogenous polypeptide expressed in normal liver tissue but lost in the liver of most HCC patients (73.1%). Its expression level is negatively associated with microvessel density ($P = 0.020$), tumor size ($P = 0.035$), and metastasis ($P = 0.016$) in HCC patients. To evaluate its potential use as a therapeutic, we constructed a recombinant adeno-associated virus carrying vastatin (rAAV-vastatin) to treat HCC in an orthotopic Buffalo rat model. rAAV-vastatin treatment significantly prolonged the median survival, inhibited tumor growth, and completely prevented metastasis in HCC-bearing rats by decreasing microvessel density and increasing tumor necrosis. No detectable toxicity in non-tumor-bearing mice was observed. To investigate its molecular mechanisms, we performed DNA microarray, western blotting assays, and bioinformatic analysis to determine its effect on global gene expression patterns and signal transduction pathways. Our results indicated that rAAV-vastatin significantly reduced genes involved in the cellular metabolism, Notch signaling, and AP-1 signaling pathways, respectively. Taken together, we demonstrated for the first time that vastatin is a novel, safe, and effective antiangiogenic therapeutic and a potential biomarker for HCC.

INTRODUCTION

Hepatocellular carcinoma (HCC) is the fifth most common cancer in the world and the third most frequent cause of cancer-related death.[1] Surgical resection is considered to be a potentially curative therapy, however, only 20% of HCC patients are eligible.[2] Nonsurgical treatments, including transcatheter arterial chemoemobolization and radiofrequency ablation have been widely used in patients with unresectable HCC.[3] However, they are not indicated for patients with advanced HCC. Chemotherapy is an option, but, the toxicity often outweighs the benefits.[4] Therefore, development of new therapeutics is urgent.

HCC has been characterized as a hypervascular tumor, which was used as a radiological feature of diagnosis.[5] Intensive staining of microvessels[6] as well as elevated expression of angiogenic factors, including vascular endothelial growth factor (VEGF) and hypoxia-inducible factor 1α (HIF1α), have been demonstrated.[7,8] These characteristics make it a potential target for antiangiogenic therapy. Currently, the most established approach for limiting tumor angiogenesis is the blockade of VEGF pathway, such as a ligand-trapping monoclonal antibody (bevacizumab) and kinase inhibitors (sorafenib and sunitinib).[9–11] Sorafenib (Nexavar, a small molecular inhibitor), approved in United States by US Food and Drug Administration (FDA) for clinical use, has been shown to prolong overall survival and time to progression in patients with advanced HCC.[12] However, because of evasive and intrinsic resistance, the benefits are transitory. There is a need for the development of new angiogenesis inhibitors targeting multiple mechanisms to circumvent resistance and reduce toxicity.[13]

The NC1 domain of collagen VIIIα1 (vastatin, **Figure 1a**) polypeptide, has been shown to inhibit the proliferation/migration of bovine aortic endothelial cells.[14] Since vastatin is derived from Collagen VIIIα1, we postulated that it may be an endogenous antiangiogenesis polypeptide. Here, we report for the first time that vastatin is readily detectable in normal liver tissues, but is deficient in the liver of most human HCC patients.

The first two authors contributed equally to this work.

Correspondence: Zan Shen, Department of Oncology, Affiliated 6th People's Hospital, Shanghai Jiaotong University, Yi Shan Road 600, Shanghai 200223, China. E-mail: sshenzzan@vip.sina.com or Marie Chia-mi Lin, Department of Oncology, Affiliated 6th People's Hospital, Shanghai Jiaotong University, Yi Shan Road 600, Shanghai 200223, China. E-mail: mcmlin@163.com
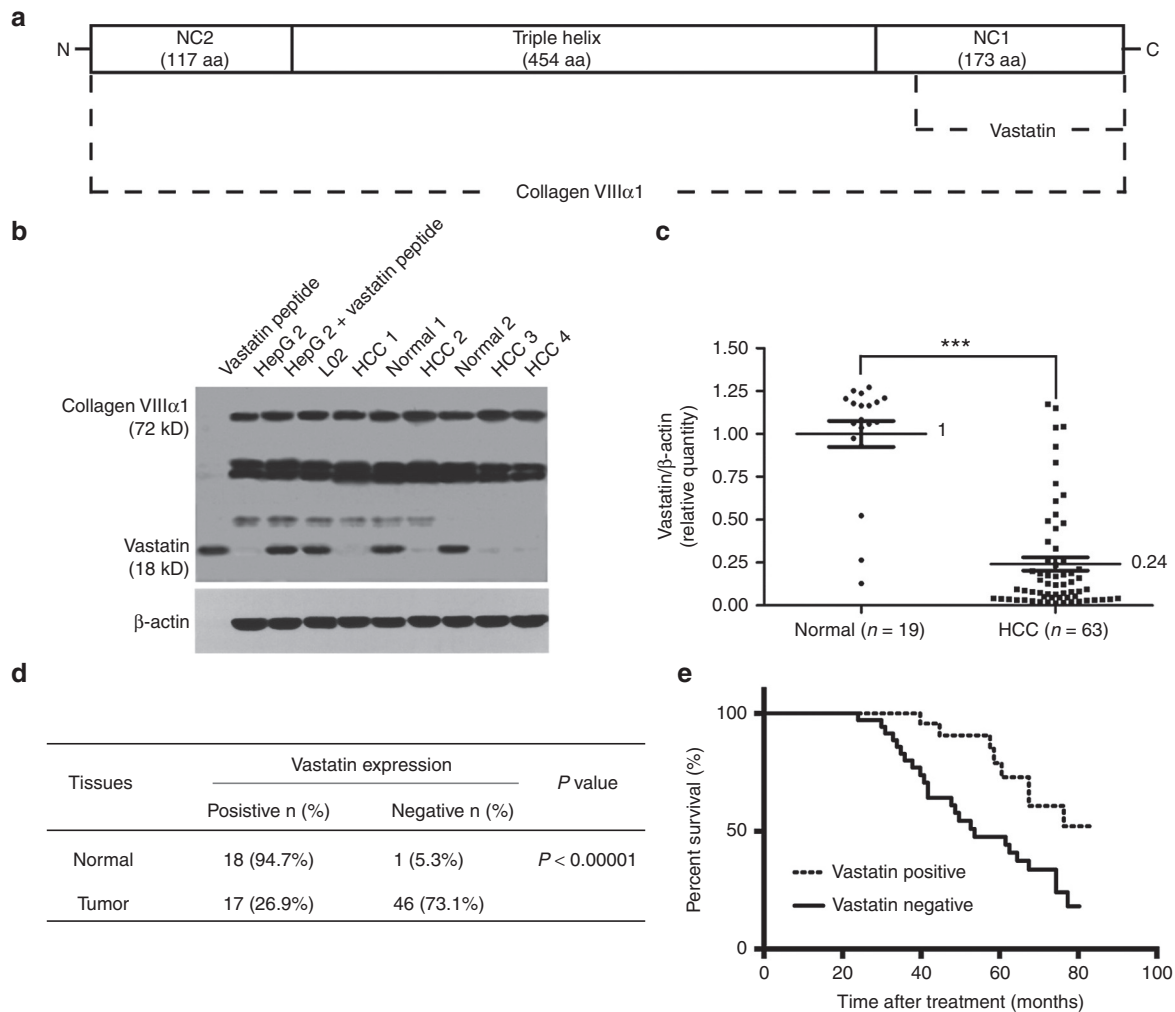
Figure 1 Vastatin expression level is significantly reduced in HCC cell line and patient specimens as compared to normal liver cell line and liver samples. (**a**) Schematic representation of the α1 chain of collagen VIII. vastatin encodes a polypeptide of 164 amino acid residues corresponding to the fragment of the NC1 Domain of Collagen VIIIα1. (**b**) The expression of vastatin in human HCC HepG2 cell line, HepG2+vastatin peptide, normal liver L02 cell line, normal liver samples, and HCC patient specimens was determined by western blotting assays. The heterologous vastatin peptide expressed in *Escherichia coli* was used as a positive control. (**c**) Western blotting results of vastatin in normal and HCC specimens were quantified by QUANTITY ONE software. The relative level was first normalized against β-actin internal control and then normalized against the average of the 19 control normal liver samples. (**d**) The expression of vastatin in normal and tumor liver tissues. Negative vastatin expression denotes the expression level is under 24.2% of the average control value. (**e**) Kaplan-Meier and log-rank test analysis indicated that patients with negative vastatin expression have shorter 5 years overall survival than those with positive expression.

Furthermore, its expression level is negatively associated with HCC tumor size and metastasis. To test its efficacy as a therapeutic, we constructed an adeno-associated virus (AAV) vector carrying the vastatin gene (rAAV-vastatin) and demonstrated that administration of rAAV-vastatin to HCC-bearing rats produced sustained expression, decreased tumor microvessel density, prolonged survival, reduced tumor growth, and completely prevented metastasis. To understand its mechanisms, we showed that rAAV-vastatin infection suppressed the proliferation, migration and tube formation of mouse microvascular endothelial cells (MECs) *in vitro*. DNA microarray, western blotting, and bioinformatics studies further indicated that rAAV-vastatin acted through three major signal transduction pathways in MECs. It significantly inhibited the expressions of: the metabolism signaling pathway member Pck1; the Notch signaling pathway member JAG2; and the AP-1 signaling pathway members c-Fos, matrix

metalloproteinase (MMP2), and MMP9. These results suggested for the first time that vastatin is a novel, safe, and effective antiangiogenic therapeutic and potential biomarker for HCC.

RESULTS

Vastatin is an endogenous polypeptide significantly reduced in human HCC tumor tissues and negatively correlated with microvessel density, tumor size, and metastasis in patients with HCC

Since vastatin is a polypeptide derived from natural collagen VIIIα1 protein (**Figure 1a**), we postulated that it may be an endogenous antiangiogenesis polypeptide, and the loss of vastatin expression may contributed to HCC carcinogenesis. As expected, immunohistochemical studies or quantitative polymerase chain reaction (qPCR) analysis on human tissue samples failed to distinguish vastatin from Collagen VIIIα1. Therefore, the specificity

Table 1 Patient demographics and Vastatin expressions in clinical subgroups

Characteristic	Vastatin expression		
	Positive *n* (%)	Negative *n* (%)	*P* value
Sex			
Male	9 (28.1)	23 (71.9)	0.48
Female	8 (25.8)	23 (74.2)	
Age			
<50 years	11 (30.6)	25 (69.4)	0.33
≥50 years	6 (22.2)	21 (77.8)	
Histological type			0.061
MD	10 (33.3)	20 (66.7)	
PD	6 (18.8)	26 (81.2)	
Unknown	1 (100)	0	
Tumor size			0.022*
≤5 cm	12 (44.4)	15 (55.6)	
>5 cm	5 (13.9)	31 (86.1)	
Metastasis			0.005*
Negative	14 (48.3)	15 (51.7)	
Positive	3 (8.8)	31 (91.2)	
Treatment			0.59
CMT	5 (21.7)	18 (78.3)	
No CMT	12 (30.0)	28 (70.0)	
HBs Ag			0.090
Negative	9 (69.2)	14 (30.8)	
Positive	7 (18.4)	31 (81.6)	
Unknown	1 (50.0)	1 (50.0)	
Anti-HCV			0.67
Negative	6 (24.0)	19 (76.0)	
Positive	9 (25.0)	27 (75.0)	
Unknown	1 (100)	0	

Negative vastatin expression denotes that the expression level is fewer than 24% of the control value.
anti-HCV, antibody to hepatitisC virus; CMT, chemotherapeutic treatment; HBsAg, hepatitisB surface antigen; M, methylated; MD, moderate-differentiation; PD, poor-differentiation; U, unmethylated.
*Statistically significant association ($P < 0.05$).

and expression level of endogenous vastatin was determined by western blotting assays (**Supplementary Figure S1**). As shown in **Figure 1b**, the small 18 kD polypeptide vastatin is nearly undetectable or weakly detectable in the human HCC HepG 2 cell line and human HCC patient specimens, while it is readily detectable in normal liver L02 cells and normal human liver samples. Meanwhile, the immunostainings for Collagen VIIIα1 protein (72 kD) and partially degraded longer proteins were unchanged. The relative intensity of the vastatin band from western blotting assays was quantified by QUANTITY-ONE software (**Supplementary Figure S2**). As shown in **Figure 1c**, the average expression level of vastatin from 63 human HCC patient specimens is only 24.2% of that from 19 normal human liver samples

Table 2 Factors independently associated with Vastatin expression in hepatocellular carcinoma

| Variable	Vastatin expression		Logistic regression analysis		
	Positive No. (%)	Negative No. (%)	RR	95% confidence interval	*P* value
Tumor size (cm)					
≤5	12 (44.4)	15 (55.6)	1.000		
>5	5 (13.9)	31 (86.1)	3.106	1.182–8.130	0.035
Edmondson-Steiner grade					
I-II	13 (43.3)	17 (56.7)	1.000		
III-IV	4 (12.1)	29 (87.9)	2.711	1.134–6.442	0.023
Metastasis					
No	14 (48.3)	15 (51.7)	1.000		
Yes	3 (8.8)	31 (91.2)	5.523	2.138–12.625	0.016

RR, relative risk.

($P < 0.001$). Therefore, we defined the expression-level of vastatin under 24.2% of the normal average as "vastatin negative"; and above 24.2% as "vastatin positive". As shown in **Figure 1d**, 73.1% (46 out of 63) of HCC patient specimens were vastatin negative, whereas only 5.3% (one out of 19) of normal liver tissues was vastatin negative. In addition, Kaplan-Meier method and log-rank test analysis demonstrated that patients with negative vastatin expression have shorter 5 years overall survival than those with positive expression (**Figure 1e**).

The patient demographics and vastatin expressions in clinical subgroups are shown in **Table 1**. Vastatin expression is not associated with gender, age, histological type, chemotherapy treatment, HBsAg, or HCV status. Multivariate logistic regression analysis indicated that negative vastatin expression correlated with microvessel density longer than 40 μmol/l ($P = 0.02$), tumor size larger than 5 cm in diameter ($P = 0.035$), metastases ($P = 0.016$) and Edmondson-Steiner III-IV high grade ($P = 0.023$, **Table 2**).

Administration of rAAV-vastatin significantly prolonged survival, inhibited tumor growth, and completely prevented metastasis *in vivo* in HCC-bearing rats

Using the orthotopic Buffulo rat model of HCC, we showed that rAAV-vastatin or rAAV-Endostatin treatments significantly prolonged the median survival time to 54 and 42 days, respectively, from 29 and 26 days ($P < 0.01$; **Figure 2a**) for the PBS- and rAAV-EGFP-treated groups. The average volume of primary tumors from the rAAV-vastatin and rAAV-Endostatin treatment groups were similar, and significantly smaller than that of the control groups at day 21 post-treatment ($P < 0.01$; **Figure 2b**). The liver, lung, and peritoneal metastasis were evaluated immediately after the death of each animal. No metastasis was observed in the rAAV-vastatin-treated rats (**Figure 2c**, middle panel), whereas small number of metastasis were found in rAAV-Endostatin-treated rats (**Figure 2c** lower panel), and multiple metastatic tumor nodules were observed in the control groups (**Figure 2c**, upper panel). The statistical results are shown in **Figure 2d**.
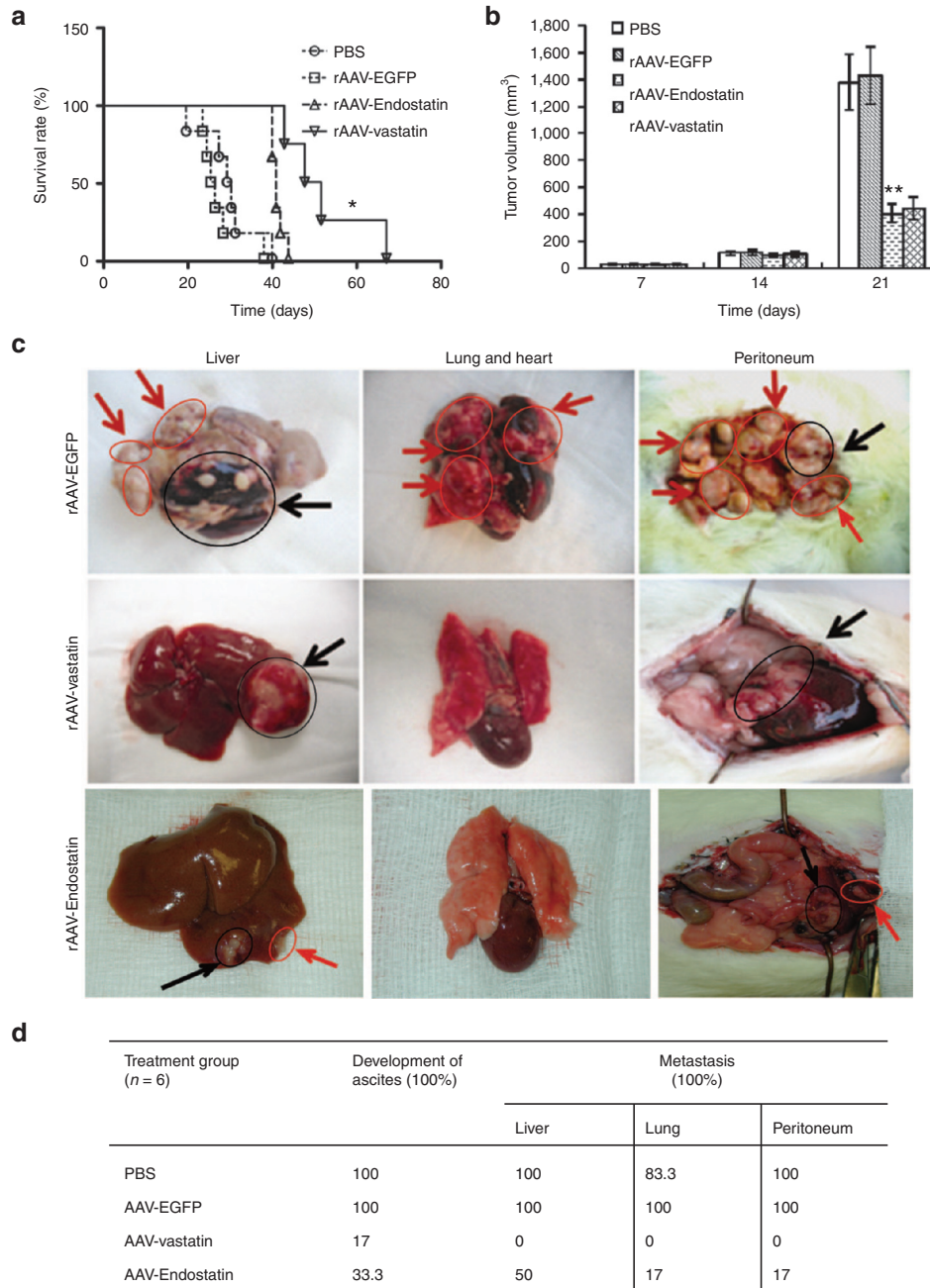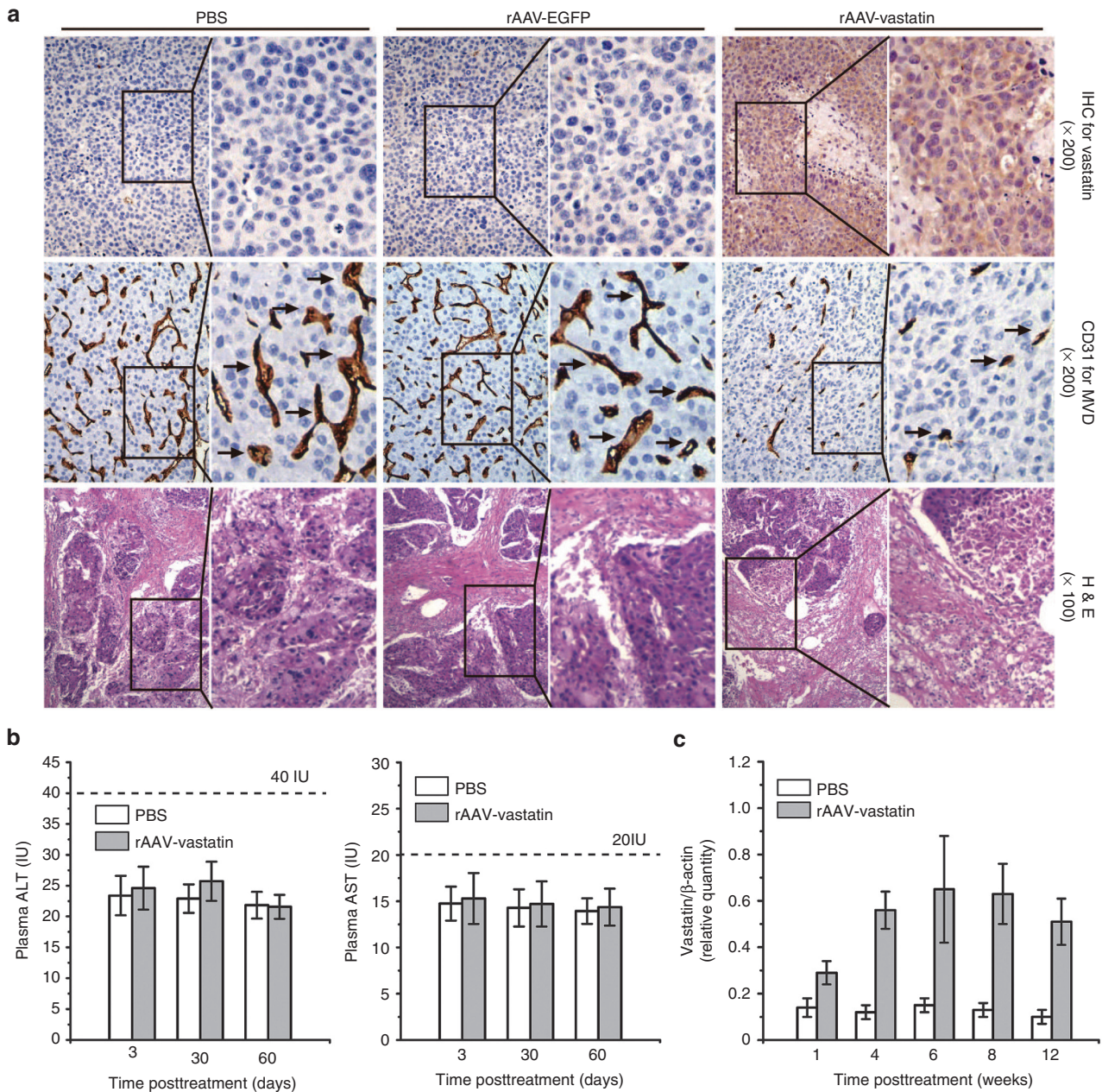
Figure 2 Administration of rAAV-vastatin significantly prolonged survival, inhibited tumor growth, and completely prevented metastasis in HCC-bearing rats. (a) Survival curves of HCC-bearing rats. rAAV-vastatin or rAAV-Endostatin treatments significantly prolonged the median survival time to 54 and 42 days, respectively, from 29 and 26 days for the PBS- and rAAV-EGFP-treated groups (*P < 0.01). (b) The primary tumor size in the rAAV-vastatin or rAAV-Endostatin treatment group was significantly smaller than that in the control groups on day 21 post-treatment (**P < 0.01). (c) Metastasis to liver, lung and peritoneum at the time of death, in the control (upper panel), rAAV-vastatin-treated (middle panel), and rAAV-Endostatin (lower panel) treated rats. Black arrow, primary tumor. Red arrow, metastasis. (d) Effects of rAAV-vastatin or rAAV-Endostatin treatment on the development of ascites and liver/lung/peritoneal metastasis, as observed at the time of death. Values represent mean ± SD. Significant difference was analyzed by using one-way analysis of variance with multiple comparisons. **P < 0.01 significantly different from the rAAV-EGFP-treated and PBS-treated group.

Sustained expression of vastatin decreased microvessel density and increased tumor tissue necrosis in HCC-bearing rats

By immunohistochemical analysis, we showed that injections of rAAV-vastatin but not PBS or rAAV-EGFP, had produced a sustained expression of vastatin around the blood vessels in the liver and tumor tissues, at 21-day postadministration (Figure 3a, top panel). Immunohistochemical analysis of microvessel density (Figure 3a, middle panel) demonstrated a significantly lower level of CD31+ staining (mircovessel density, 11 ± 1.3; P < 0.01) in the rAAV-vastatin treatment group as compared to PBS (29.67 ± 1.7) and rAAV-EGFP (30.50 ± 2.4).

Figure 3 rAAV-vastatin administration produced sustained expression of vastatin, decreased microvessel density, and increased tumor tissue necrosis in the HCC-bearing rats. (**a**) HCC-bearing rats were sacrificed on day 21 post-treatment. Upper panel, immunohistochemical (IHC) staining showed vastatin protein expression (brown color) in the liver, tumor tissues, and around blood vessels of the rAAV-vastatin treated rats. In addition, necrosis was found in parts of tumor tissue treated with rAAV-vastatin. Middle panel, IHC staining of CD31 for assessing mircovessel density. Arrows, CD31-positive cells. Lower panel, H&E staining for necrotic area in tumor tissues. Large area of necrosis was found in tumor tissue treated with rAAV-vastatin. (**b**) Plasma levels of ALT (left panel) and AST (right panel) in normal rats treated with ten-fold therapeutic dosage rAAV-vastatin or PBS on day 3, 30, and 60 post-treatment ($n = 6$ per group). The maximum values of normal reference of plasma tests are 40 IU (ALT) and 20 IU (AST). (**c**) Plasma vastatin levels as determined by western blotting after a therapeutic dose of rAAV-vastatin injection at week 1, 4, 6, 8, and 12.

H&E staining (**Figure 3a**, lower panel) showed that rAAV-vastatin induced large areas of necrosis in the primary tumor tissues, whereas only a few necrotic areas were observed in the control groups. We also showed that rAAV-vastatin treatment had no detectable effect on normal liver vasculature in healthy rats (**Supplementary Figure S3a**).

Study of toxicity in healthy rats or mice treated with rAAV-vastatin

The potential toxicity of the portal vein injection of rAAV-vastatin was examined in healthy Buffulo rats and C57 mice. At single animal studies, a single 10-fold effective therapeutic dosage (4.4×10^{13} vg/kg; or 1.2×10^{12} vg/mouse; 1.2×10^{13} vg/rat) did not produce
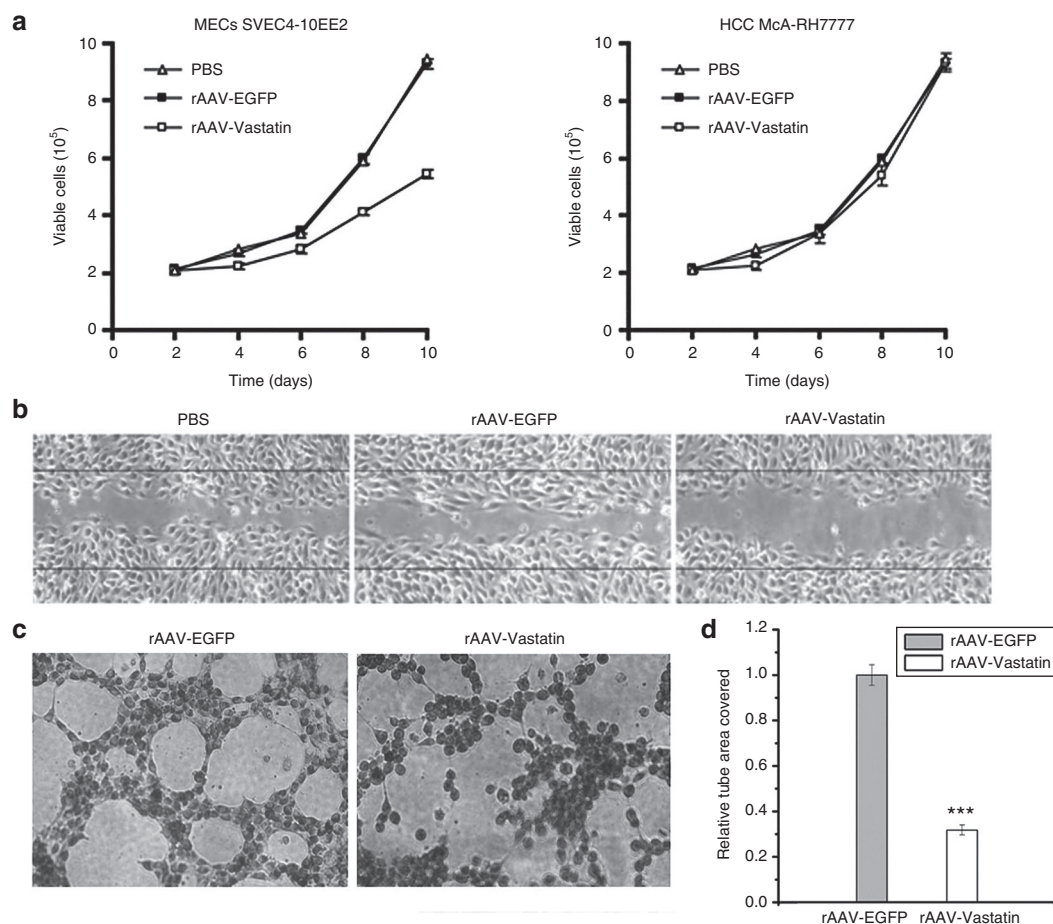
Figure 4 rAAV-vastatin effectively inhibited the proliferation, migration, and microvessel tube formation of microvascular endothelial cells (MECs). (**a**) MTT assay to determine viable cell numbers. MECs SVEC4-10EE2 (left) and HCC McA-RH7777 (right) cells were treated with rAAV-vastatin, rAAV-EGFP, or PBS. (**b**) Wound-healing assay to determine cell migration rate. SVEC4-10EE2 MECs were infected with rAAV-vastatin, rAAV-EGFP, or PBS (**c**) Tube formation assay by the EcMatrixTM method. SVEC4-10EE2 MECs were infected with rAAV-vastatin or rAAV-EGFP. (**d**) Bar graph shows the relative tube area covered.

obvious toxicity in either rat or mice. In medium-term toxicity study in mice, 10-fold therapeutic dosage of rAAV-vastatin ($n = 6$ per group), did not cause significant changes in plasma ALT or AST levels on days 3, 30, and 60 postinjection as compared to the PBS-treated mice (**Figure 3b**). We also demonstrated that a therapeutic dose of rAAV-vastatin injection ($n = 6$ per group) produced a sustained vastatin expression in the plasma as determined by western blotting assay. The plasma vastatin level peaked at 6 weeks (42 days) postinjection, and maintained at high level for more than 12 weeks (**Figure 3c**). For long-term toxicity studies, rats were given therapeutic dosage of rAAV-vastatin or phosphate-buffered saline(PBS). Two milliliters of blood were taken on day 3, 30, 60, and 75 postinjection, and liver function (Alanine Aminotransferase (ALT); Aspartate Aminotransferase (AST)), renal function (Cre, Blood Urea Nitrogen (BUN)), hematopoiesis (White Blood Cell Count (WBC); Hb, Platelet (PLT)), cholesterolemia (cholesterol), and blood sugar (glucose) were determined. There was no significantly elevated plasma ALT, AST, Cre, and BUN levels during the time course (**Supplementary Figure S3b–d**). In all toxicity studies, no

significant changes in body weight, gross appearance, and behavior were noticed in animals.

rAAV-vastatin infection effectively inhibited the proliferation, migration, and microvessel tube formation activities in MECs

To study how rAAV-vastatin exerts the antitumor activity, we examined the effect of rAAV-vastatin infection on microvascular-endothelial SVEC4-10EE2 cells and rat HCC McA-RH7777 cells. rAAV-vastatin efficiently transfected both cells and produced vastatin (**Supplementary Figure S4**). rAAV-vastatin infection decreased the number of viable MECs SVEC4-10EE2 cells significantly (to 53.3% of the control, $P < 0.01$) at 10 days after infection, (**Figure 4a**), and reduced the migration rate of MEC cells (**Figure 4b**, wound healing assay), whereas it had no effect on the HCC McA-RH7777 cells. In addition, it reduced the relative microvessel tube formation (EcMatrix assay) to 31% of the control PBS and rAAV-EGFP treatment groups (**Figure 4c**).
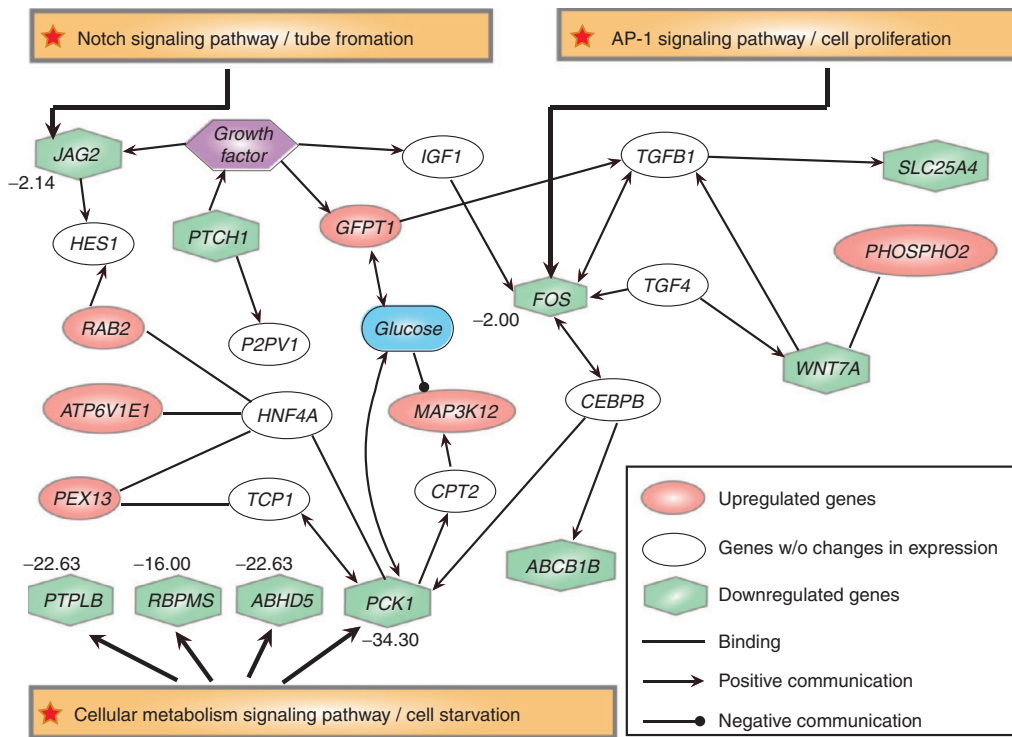
Figure 5 rAAV-vastatin signaling network. Three major mechanisms are involved in the actions of vastatin in SVEC4-10EE2 microvascular endothelial cells. vastatin inhibited (1) AP-1 activity and cell proliferation by down-regulation of the Fos gene; (2) Notch signaling activity and tube formation via the down-regulation of the JAG2 gene; and (3) metabolisms leading to energy starvation through the down-regulation of the PCK1, ABHD5, RBPMS, and PTPLB genes. This signaling network was generated by the software PathwayArchitect.

Effects of rAAV-vastatin infection on global gene expression profile in MECs

To understand the molecular mechanisms of rAAV-vastatin, we determined its effect on the global gene expression profile in MECs SVEC4-10EE2 cells at 48 hours after infection, using Affymetrix DNA microarrays technology. Our results showed that 30 genes were upregulated and 30 downregulated for more than twofold (**Supplementary Table S1**). To our surprise, vastatin most profoundly downregulated four metabolic genes, phosphoenolpyruvate carboxyknoase-1 (Pck1, -34.3-fold reduction), abhydrolase domain containing 5 (Abhd5, -22.6 reduction), protein tyrosine phosphatase-like member b (Ptplb, -16.0 reduction), and RNA binding protein gene with multiple splicing (Rbpms, -16.0 reduction), which are involved in the regulation of carbohydrate, lipid, protein, and mRNA metabolisms, respectively. The dysregulated genes could be assigned to 15 different functional groups (**Supplementary Figure S5**). Within the regulated genes, "transport" molecules and "transcription factors" were upregulated more often, while, "signal-transduction receptors" and "metabolism" genes were downregulated more often.

### rAAV-vastatin infection markedly downregulated three major signaling pathways in MECs

PathwayArchitect were employed to generate putative signaling networks based on the expression profiling data. Three major networks were identified (**Figure 5**). They are downregulations of (i) metabolisms, (ii) Notch signaling, and (iii) AP-1 signaling. To validate these signal-pathway networks, RT-PCR and western blotting assays were performed to confirm the changes of key genes. Our results demonstrated that rAAV-vastatin significantly downregulated the mRNA and protein levels of the key metabolism gene Pck1 (**Figure 6a**) to 15 and 50%, respectively, at 24 hours after infection and maintained the low level at 72 hours. It reduced the mRNA and protein levels of the Notch signaling gene JAG2 (jagged 2, **Figure 6b**) to 62 and 85%, respectively at 24 hours, and to 38 and 50%, at 72 hours. It decreased the protein levels of the AP-1 signal gene c-Fos to 90, 70, and 30%, at 24, 48, and 72 hours postinfection, respectively. In contrast, c-Fos partner c-Jun or Jun-B, were not affected (**Figure 6c**). The protein levels of c-Fos downstream angiogenesis-associated genes MMP2 and MMP9 were also significantly downregulated to 40% at 72 hours postinfection, whereas MMP1, uPA, or VEGF exhibited no significant change (**Figure 6d**). Based on the existing knowledge of these signal pathways, we postulate that rAAV-vastatin infection leads to (i) cell starvation through the inhibition of metabolisms, (ii) reduced cell proliferation and migration through the inhibition of AP-1 signaling pathway, and (iii) reduced angiogenesis by inhibiting tube formation through the Notch signaling pathway (**Figure 5**).

DISCUSSION

In the present study, we report for the first time that vastatin is a naturally occurring antiangiogenic polypeptide, present at a readily detectable level in normal liver, and lost in most of the HCC tumor tissues. Statistical analysis indicated that negative vastatin expression independently correlated with tumor size larger than
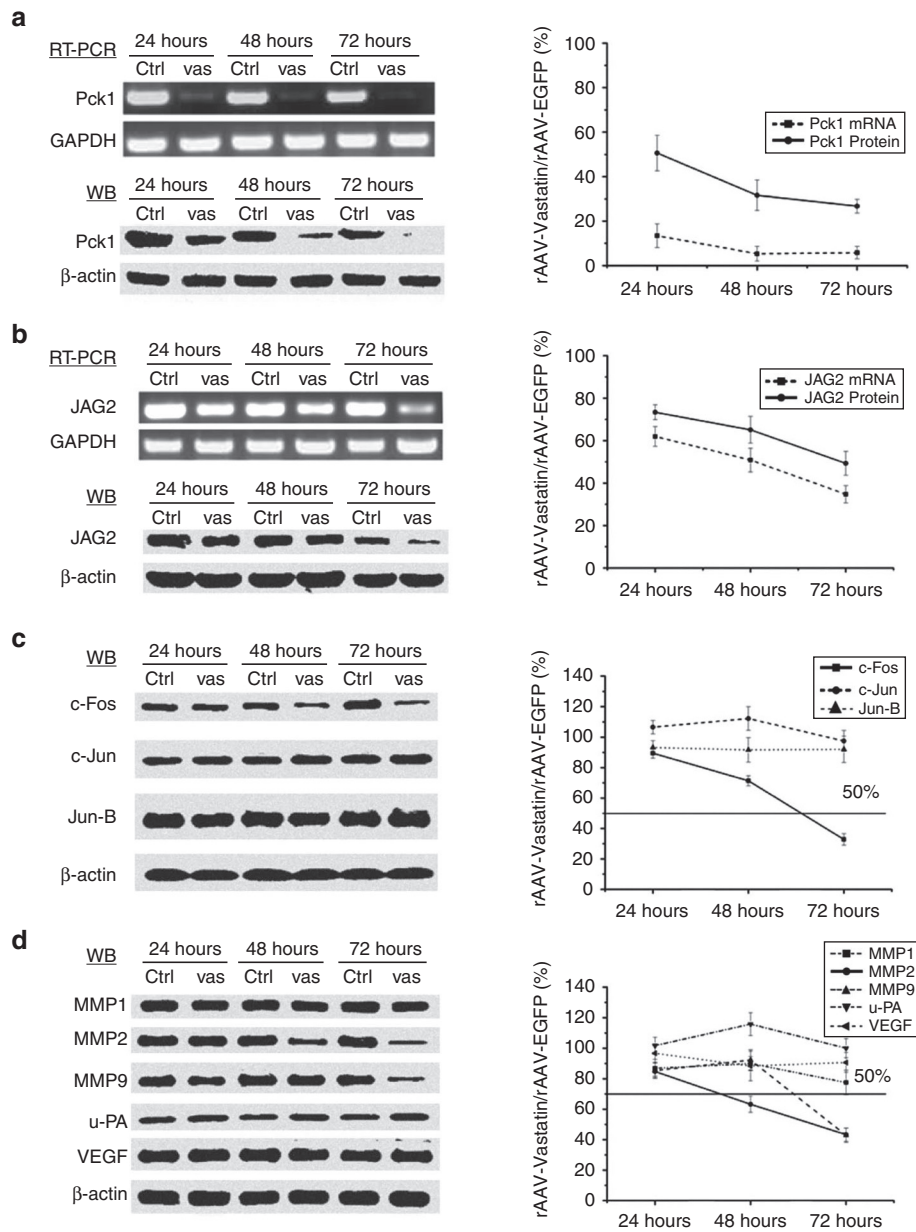
Figure 6 Validation of rAAV-vastatin induced downregulation of key genes involved in three major signaling pathways in microvascular endothelial cells (MECs). RT-PCR and western blotting (WB) assays were conducted to determine the mRNA and protein expressions, respectively, of key genes over one, two, and three days after rAAV-vastatin infection in SVEC4-10EE2 MECs. (**a**) the metabolism-associated genes Pck1, (**b**) the Notch signaling gene JAG2, (**c**) the AP-1 complex genes c-Fos, and (**d**) the AP-1 down-stream MMP2 and MMP9. "Ctrl" indicates "control" and "Vas" indicates "rAAV-vastatin".

5 cm in diameter, metastases and Edmondson-Steiner III-IV high grade. Further studies with longer cohorts and refined statistics will be needed in order to fully establish the predictive value of vastatin as a biomarker for HCC.

It is not known how vastatin is lost in HCC tumors. Because the other longer length Collagen VIIIα1 proteins were not affected, suggesting that the defects are likely in the machinery releasing vastatin. The lysosomal enzymes Cathepsins (CTSD or CTSL) has been shown to be the key peptidase to release antiangiogenic fragments, such as Endostatin (NC1 domain of collagen XVIII), 16K prolactin (16 kD N-terminal fragment of

prolactin), and Angiostatin (38 kD internal fragment of plasminogen).[15] We conducted an *in silico* analysis and found that CTSL expression level is significantly reduced in HCC, and the reduced expression is associated with venous metastasis (*P* < 0.05, GEO Profile, **Supplementary Table S2**). In addition, the MMPs have also been shown to degrade collagen and to generate anti-angiogenic fragments, such as Endostatin, Arresten (NC1 domain of collagen IV a1), Canstatin (NC1 domain of collagen IV a2), and Tumstatin (NC1 domain of collagen IV a3).[16–18] The roles of CTSL and MMPs on the production of vastatin warrant further investigations.

Collagen VIII is not known to link to any genetic disease. The crystal structure of NC1 domain trimmers of mouse Col8a1 (Collagen VIIIα1) has been solved at 1.9 Å resolution.[19] Col8a1 and Col8a2 (Collagen VIIIα2) null mice had been reported to be viable, fertile, and show no major abnormalities.[20] Detailed studies revealed that lack of collagen VIII leads to an abnormal anterior chamber of the eye, and attenuated migration/growth of the vascular smooth muscle cells.[21] After arterial injury and fibrous cap formation in atherosclerosis,[22] collagen VIII may play a role in mediating vessel wall remodeling via β1 integrin and RhoA signaling to regulate MMP-2 expression and smooth muscle cell migration.[23]

In addition to vastatin, several other endogenous angiogenic inhibitors have been reported.[24] Endostatin, the most well-characterized, has been investigated in clinical trials.[25–27] vastatin/Collagen-VIII exhibit different expression profiles as compared to Endostatin/Collagen-XVIII in liver cancers.[28] The antiangiogenesis activity of vastatin polypeptide has previously been shown to be similar to that of Endostatin *in vitro* in cell culture systems.[14,29] We compared the *in vivo* efficacy in HCC. Our results showed that rAAV-vastatin was slightly more potent than rAAV-Endostatin in reducing metastasis and prolonging median survival in the orthotopic Buffalo rat HCC model. Endostar, a rh-endostatin, has been shown to improve the tumor response rate of patients with advanced non–small-cell-lung cancer when used in combination with platinum-based chemotherapy. However, no improvement in survival rate of patients was demonstrated.[30] It is likely that vastatin and Endostatin work through different receptors. Endostatin has been shown to work through growth-factor receptors,[31–35] in particular VEGFR.[33,36,37] We conducted *in silico* analysis, and found no significant homology between vastatin and the other antiangiogenic collagen fragments, suggesting that vastatin may act *via* distinct cell surface receptor(s). It is possible that vastatin or the combination of vastatin and Endostatin may have better efficacy for the treatment of HCC.

Angiogenesis is a multi-step process including endothelial-cell proliferation, migration, basement-membrane degradation, and new-lumen organization.[38] In order to have a comprehensive view of the molecular mechanisms, we chose to employ DNA microarray study to investigate the effect of rAAV-vastatin on global gene expression profile in MECs. Our results revealed that rAAV-vastatin acted by downregulating key genes involved in AP-1, Notch signaling, and the metabolisms of carbohydrates, lipids, and proteins. The Notch signaling pathway and the AP-1 signaling pathway in tumor progression were relatively well-studied.[39,40] JAG2 and Notch-1 have been implicated in the production of IL-6, VEGF, and IGF-1 by multiple myeloma-associated stromal cells.[41] Several growth-factors and cytokines-mediated pathways including VEGF and MMPs converged at the AP-1 binding site.[42–44] However, less is understood about the significance of metabolism in cancers.

Emerging evidence has pointed to the increasingly important roles of metabolism in carcinogenesis. Several metabolic enzymes, such as pyruvate-kinase M2 isoenzyme (PKM2) and isocitrate-dehydrogenase (IDH1/2), have been shown to play pivotal roles in tumor-progression and are potential targets for anticancer therapeutics.[45] Despite the obvious fact that blood vessels carry oxygen/nutrients to all cells and should be a major factor regulating cellular metabolism, the link between endothelial-cell metabolism and angiogenesis has been largely ignored. Our data showed that at least four metabolism-associated genes Pck1, ABHD5, Ptplb, and Rbpms, involved in the metabolism of carbohydrate, lipid, protein, and mRNA, respectively.[46–49] were significantly down-regulated (**Figure 5**). Thereby suggesting that cellular metabolism signaling pathways were the major targets of rAAV-vastatin.

In conclusion, we identified vastatin as a naturally occurring antiangiogenesis polypeptide lost in HCC cells. Furthermore, rAAV-vastatin is an effective therapeutic for HCC that works through novel mechanisms, including inhibiting cellular metabolism, tube formation, and inhibiting cell proliferation and migration via the downregulation of multiple signaling pathway (**Supplementary Figure S6**). Taken together, these results demonstrate that vastatin could be a novel biomarker and rAAV-vastatin could be a novel, effective, and safe treatment for HCC. The differential mechanisms of vastatin and Endostatin suggest that these two endogenous angiogenic inhibitors could be used in combination to achieve a synergistic therapeutic effect for HCC treatment.

MATERIALS AND METHODS

Patients. Nineteen normal liver samples were obtained from patients with liver trauma due to traffic accident who underwent partial hepatectomy. The patients were diagnosed as III or IV stage of liver trauma, according to classification by American Association for the Surgery of Trauma (AAST), and without medical history of hepatopathy. The samples were taken at locations away from the trauma and on the verge of hepatic lobes or hepatic segments. The 63 tumor specimens were from HCC patients underwent surgery between 2006 and 2010 at the Department of Hepatobiliary Surgery, Taizhou Hospital, Wenzhou Medical College, Zhejiang, China. For patients with advanced HCC, biopsies were taken from the primary nodules. Tumor sizes were calculated according to Response Evaluation Criteria in Solid Tumors. Histological subtyping of the HCCs include moderately differentiated, poorly differentiated and unknown. The unknown samples indicate the cases that could be diagnosed as HCC, however, difficult to determine the subtype. There are no well differentiated HCCs in our patient population, consistent with epidemiological reports of very low percentage of well differentiated HCC in China. The written informed consent of each patient and the approval of the ethics committee of the University were obtained beforehand. The basic demographics and pathological characteristics are shown in **Table 1**.

Cell lines and cell culture. Murine tumor-derived MEC SVEC4-10EE2, rat HCC McA-RH7777, human HepG2, and LO2 cell lines were purchased from American Type Culture Collection, and maintained in Dulbecco's modified Eagle's medium (DMEM; Invitrogen, Carlsbad, CA) supplemented with 10% fetal-bovine-serum (FBS, Invitrogen) at 37 °C, 5% CO_2.

Western blotting analysis. Cell lysates were separated by 12% SDS polyacrylamide gels, transferred to Polyvinylidene Fluoride (PVDF) membranes, and probed with primary antibodies. The polyclonal anti-vastatin antibody was custom-made (Boster Biotechnical) by immunizing rabbits with purified recombinant polypeptide expressed in *Escherichia coli*. The antibody was shown by the company to have no cross-reactivity with other members of the family. By western blot, this antibody detect a 18 kD purified recombinant vastatin polypeptide, as well as several bands including a 72 kD band (likely to be collagen VIII alpha1) in HepG2 cell and normal liver tissue lysates (**Supplementary Figure S1**). Antibodies against Pck1 and JAG2 were from Abcam (Cambridge), and against c-Fos, c-Jun, Jun-B, MMP1, MMP2, MMP9, u-PA, VEGF, and β-actin were from Santa Cruz Biotechnology (Santa Cruz). The relative expression levels were quantified using QUANTITY ONE software (Bio-Rad).

Preparation of rAAV-vastatin and rAAV-Endostatin virus. Plasmids rAAV-CAG EGFP (rAAV-EGFP), rAAV-CAG-sec-Endostatin (rAAV-Endostatin) and rAAV-CAG-sec-vastatin (rAAV-vastatin) were constructed by inserting fragments encoding the EGFP, Endostatin, and vastatin into AAV2 vector (**Supplementary Figure S7**). The secretion of vastatin protein was mediated by Igk leader. Viral titer was quantified as described previously.[50]

Rat orthotopic HCC model. The buffalo rat orthotopic HCC model was established as described previously.[50] All animal studies and the experimental protocols were approved in advance by the Department of Health of the Government of Hong Kong Special Administrative Region and by the Ethic Committee on the Use of Live Animals in Teaching and Research (The Chinese University of Hong Kong). Male buffalo rats, 8 to 12 weeks old, weighing 250 to 320 g, were purchased from Charles River Laboratory. Tumor was induced by injection of 6×10^5 McA-RH7777 cells into the left lobe of the liver. At 14 days after cell injection, rats were randomly divided into three groups ($n = 15$ per group). By second laparotomy, tumors were confirmed and treated with: (i) PBS; (ii) rAAV-EGFP (total 1.2×10^{12} vg/rat, or 4.2×10^{12} vg/k); or (iii) rAAV-vastatin (total 1.2×10^{12} vg/rat) by both intratumoral (three sites around the margin and one in the center of the tumor nodule, total 0.2×10^{12} vg) and portal vein injection (1×10^{12} vg/rat). Six rats were kept for the survival study, whereas the remaining nine rats were sacrificed by an overdose of anesthesia on days 7, 14, and 21 posttreatment for plasma, tumor tissue, and organ collections. Tissues were subjected to hematoxylin and eosin (H&E) and immunohistochemical staining as described previously.[51]

Toxicity test. Toxicity was conducted in healthy male buffalo rats or C57 mice (6–8 weeks old weighing 25 to 30 g, from the Laboratory Animal Unit of the Chinese University of Hong Kong with Ethic approval). Rats or mice were given PBS or rAAV-vastatin by intraportal vein injections. For mice study, mice were sacrificed and blood collected for ALT and AST determinations. For rats study, two milliliters of blood samples were taken at indicated time and evaluated for liver function (ALT, AST), renal function (Cre, BUN), hematopoiesis (WBC, Hb, PLT), cholesterolemia (cholesterol), and blood sugar (glucose). Mice and rats were assessed daily on body weight, gross appearance, and behavior, for any signs of systemic toxicity.

Cell proliferation assay. Mouse MECs SVEC4-10EE2 or rat HCC McA-RH7777 cells (3×10^3 cells) were seeded onto 96-well plates overnight. Ten microliters of PBS, rAAV-EGFP, or rAAV-vastatin were added at a multiplicity of infection of 1×10^4, and incubated for 2, 4, 6, 8, and 10 days in DMEM with 2% FBS. MTT (3-(4,5-dimethyl-2-thiazolyl)-2,5-diphenyl-2-H-tetrazolium bromide) assays were performed, as described previously.[50]

In vitro tube formation and wound-healing assays. MECs SVEC4-10EE2 (3×10^5) were seeded onto six-well plates overnight, and treated with PBS, rAAV-EGFP, or rAAV-vastatin (multiplicity of infection = 1×10^4) in DMEM with 2% FBS for 24 hours, followed by starvation in DMEM with 0.5% FBS for 48 hours. The effect was evaluated by using the *In vitro* Angiogenesis Assay kit (Chemicon, Temecula, CA) as described previously.[50] Tube formation was quantified as relative tube-area covered.[52] Wound-healing assays were performed, as previously described.[50]

DNA microarray study. MECs SVEC4-10EE2 cells were infected with rAAV-vastatin or rAAV-EGFP for 48 hours. Total RNA were extracted, biotin-labeled, fragmented, and hybridized to the GeneChip Mouse Exon 1.0 ST Array (Affymetrix, Santa Clara, CA) using Hybridization Oven 640 (Affymetrix) in triplicate by the Genome Research Center, The University of Hong Kong. Twofold differentially expressed probe sets were identified. The signal transduction pathway analysis was conducted using the software PathwayArchitect.

The mRNA and protein expression were validated by reverse transcription-PCR (RT-PCR) and western-blotting assays, respectively. The following primer sequences were used: Pck1 (forward 5′-GCTC TGAGGAGGAGAATGG-3′; Reverse 5′-TGC TCTTGGGTGACGATAA C-3′); JAG2 (Forward 5′-CAAGTTCTGTGACGAGTG TGTCCC-3′; Reverse 5′-TTGCCCAAGTAGCCATCTGG-3′); and GAPDH (Forward 5′-GAATCTACTGGCGTCTTCACC-3′; Reverse 5′-GTCATGAGCCCT TCCACG ATG C-3′).

Immunohistochemical staining and measurement of microvessel density. The paraffin-embedded tissue blocks were sectioned for immunohistochemical staining. Paraffinembedded tissue specimens were sectioned, deparaffinized in xylene and rehydrated. Antigenic retrieval was processed with sodium citrate. The sections were then incubated in H_2O_2 (3%) for 10 minutes, blocked in 1% bovine serum albumin for 60 minutes and incubated with indicated antibody at 4 °C overnight. After incubation with the secondary antibody for 60 minutes, specimens were incubated with H_2O_2-diaminobenzidine until the desired stain intensity was developed. Sections were then counterstained with hematoxylin, dehydrated, and mounted.

Microvessel density was measured as described previously.[53] Briefly, tissues were fixed with 10% formalin, embedded in paraffin and subjected to HE staining. Any vessels with brown staining in the tumor tissues were considered positive. Any brown-stained endothelial cell or cell cluster was regarded as one vessel. For special types of microvessel with a large vascular lumen and a relatively small number of vessels per unit area, a length of 40 μmol/l was regarded as one mircovessel density value, as described previously.[54] All immunohistochemical staining was evaluated and scored by at least two independent pathologists.

Statistical analysis. Animal survival was analyzed by a log-rank test using the GraphPad Prism software (GraphPad Software, San Diego, CA). Correlation was analyzed by multivariate logistic regression. Comparison was conducted by one-way analysis of variance or a two-tailed Student's *t*-test (MS Excel). $P < 0.05$ was considered statistically significant.

SUPPLEMENTARY MATERIAL
Figure S1. The specificity of anti-vastatin antibody was validated by Western blot.
Figure S2. The relative expression level of vastatin in each individual HCC patients specimens (n = 63) and normal liver samples (n = 19).
Figure S3. rAAV-vastatin did not produce obvious toxicity in rat.
Figure S4. rAAV serotype 2 could efficiently transduce MECs and McA-RH7777 cells.
Figure S5. Functional categorization of genes differentially expressed by rAAV-vastatin treatment in mouse microvascular endothelial cells.
Figure S6. rAAV-vastatin exerted its anti-angiogenic activities by down-regulation of three angiogenic signaling pathways in MECs.
Figure S7. Structure of rAAV-vastatin.
Table S1. The list of differentially expressed genes after rAAV-Vastatin treatment.
Table S2. The expression levels of CTSD in normal liver tissue and HCC with or without metastasis according to GEO Profile.

AUTHOR CONTRIBUTION
Conception and design: Z.S., Z.F., H-F.K., and M.C.L.; conduct experiments: Z.S., C.Y., Z.W., H.Y., D.M., F.L., and Y.L.; analysis and interpretation of data: H.Z., Y-J.S., G.L., W.J., and X.W.; drafting the article and final approval of the version to be published: Z.S., M.C.L., Z.W., W.S.P., and X-W.B.

REFERENCES

1. Sherman, M (2010). Epidemiology of hepatocellular carcinoma. *Oncology* **78 Suppl 1**: 7–10.
2. Hou, YB, Chen, MH, Yan, K, Wu, JY and Yang, W (2009). Adjuvant percutaneous radiofrequency ablation of feeding artery of hepatocellular carcinoma before treatment. *World J Gastroenterol* **15**: 2638–2643.
3. Biolato, M, Marrone, G, Racco, S, Di Stasi, C, Miele, L, Gasbarrini, G et al. (2010). Transarterial chemoembolization (TACE) for unresectable HCC: a new life begins? *Eur Rev Med Pharmacol Sci* **14**: 356–362.
4. Ueda, H, Fukuchi, H and Tanaka, C (2012). Toxicity and efficacy of hepatic arterial infusion chemotherapy for advanced hepatocellular carcinoma (Review). *Oncol Lett* **3**: 259–263.
5. Zeng, W, Gouw, AS, van den Heuvel, MC, Zwiers, PJ, Zondervan, PE, Poppema, S et al. (2008). The angiogenic makeup of human hepatocellular carcinoma does not favor vascular endothelial growth factor/angiopoietin-driven sprouting neovascularization. *Hepatology* **48**: 1517–1527.
6. Poon, RT, Ng, IO, Lau, C, Yu, WC, Yang, ZF, Fan, ST et al. (2002). Tumor microvessel density as a predictor of recurrence after resection of hepatocellular carcinoma: a prospective study. *J Clin Oncol* **20**: 1775–1785.
7. Takino, J, Yamagishi, S and Takeuchi, M (2012). Glycer-AGEs-RAGE signaling enhances the angiogenic potential of hepatocellular carcinoma by upregulating VEGF expression. *World J Gastroenterol* **18**: 1781–1788.
8. Kong, J, Kong, L, Kong, J, Ke, S, Gao, J, Ding, X et al. (2012). After insufficient radiofrequency ablation, tumor-associated endothelial cells exhibit enhanced angiogenesis and promote invasiveness of residual hepatocellular carcinoma. *J Transl Med* **10**: 230.
9. Kubota, Y (2012). Tumor angiogenesis and anti-angiogenic therapy. *Keio J Med* **61**: 47–56.
10. Hoang, T, Huang, S, Armstrong, E, Eickhoff, JC and Harari, PM (2012). Enhancement of radiation response with bevacizumab. *J Exp Clin Cancer Res* **31**: 37.
11. Lai, SL, Cheah, SC, Wong, PF, Noor, SM and Mustafa, MR (2012). *In vitro* and *in vivo* anti-angiogenic activities of Panduratin A. *PLoS ONE* **7**: e38103.
12. Jayson, GC, Hicklin, DJ and Ellis, LM (2012). Antiangiogenic therapy–evolving view based on clinical trial results. *Nat Rev Clin Oncol* **9**: 297–303.
13. Bergers, G and Hanahan, D (2008). Modes of resistance to anti-angiogenic therapy. *Nat Rev Cancer* **8**: 592–603.
14. Xu, R, Yao, ZY, Xin, L, Zhang, Q, Li, TP and Gan, RB (2001). NC1 domain of human type VIII collagen (alpha 1) inhibits bovine aortic endothelial cell proliferation and causes cell apoptosis. *Biochem Biophys Res Commun* **289**: 264–268.
15. Piwnica, D, Fernandez, I, Binart, N, Touraine, P, Kelly, PA and Goffin, V (2006). A new mechanism for prolactin processing into 16K PRL by secreted cathepsin D. *Mol Endocrinol* **20**: 3263–3278.
16. Genersch, E, Hayess, K, Neuenfeld, Y and Haller, H (2000). Sustained ERK phosphorylation is necessary but not sufficient for MMP-9 regulation in endothelial cells: involvement of Ras-dependent and -independent pathways. *J Cell Sci* **113 Pt 23**: 4319–4330.
17. Ortega, N and Werb, Z (2002). New functional roles for non-collagenous domains of basement membrane collagens. *J Cell Sci* **115**(Pt 22): 4201–4214.
18. Mott, JD and Werb, Z (2004). Regulation of matrix biology by matrix metalloproteinases. *Curr Opin Cell Biol* **16**: 558–564.
19. Kvansakul, M, Bogin, O, Hohenester, E and Yayon, A (2003). Crystal structure of the collagen alpha1(VIII) NC1 trimer. *Matrix Biol* **22**: 145–152.
20. Hopfer, U, Fukai, N, Hopfer, H, Wolf, G, Joyce, N, Li, E et al. (2005). Targeted disruption of Col8a1 and Col8a2 genes in mice leads to anterior segment abnormalities in the eye. *FASEB J* **19**: 1232–1244.
21. Adiguzel, E, Hou, G, Mulholland, D, Hopfer, U, Fukai, N, Olsen, B et al. (2006). Migration and growth are attenuated in vascular smooth muscle cells with type VIII collagen-null alleles. *Arterioscler Thromb Vasc Biol* **26**: 56–61.
22. Lopes, J, Adiguzel, E, Gu, S, Liu, SL, Hou, G, Heximer, S et al. (2013). Type VIII collagen mediates vessel wall remodeling after arterial injury and fibrous cap formation in atherosclerosis. *Am J Pathol* **182**: 2241–2253.
23. Adiguzel, E, Hou, G, Sabatini, PJ and Bendeck, MP (2013). Type VIII collagen signals via ß1 integrin and RhoA to regulate MMP-2 expression and smooth muscle cell migration. *Matrix Biol* **32**: 332–341.
24. Ribatti, D (2009). Endogenous inhibitors of angiogenesis A historical review. *Leukemia Res* **33**: 638–644.
25. Thomas, JP, Arzoomanian, RZ, Alberti, D, Marnocha, R, Lee, F, Friedl, A et al. (2003). Phase I pharmacokinetic and pharmacodynamic study of recombinant human endostatin in patients with advanced solid tumors. *J Clin Oncol* **21**: 223–231.
26. O'Reilly, MS, Boehm, T, Shing, Y, Fukai, N, Vasios, G, Lane, WS et al. (1997). Endostatin: an endogenous inhibitor of angiogenesis and tumor growth. *Cell* **88**: 277–285.
27. Herbst, RS, Hess, KR, Tran, HT, Tseng, JE, Mullani, NA, Charnsangavej, C et al. (2002). Phase I study of recombinant human endostatin in patients with advanced solid tumors. *J Clin Oncol* **20**: 3792–3803.
28. Musso, O, Rehn, M, Théret, N, Turlin, B, Bioulac-Sage, P, Lotrian, D et al. (2001). Tumor progression is associated with a significant decrease in the expression of the endostatin precursor collagen XVIII in human hepatocellular carcinomas. *Cancer Res* **61**: 45–49.

29. Zhang, L, Shen, X, Lu, Q, Zhou, Q, Gu, J, Gan, R et al. (2012). A potential therapeutic strategy for inhibition of ocular neovascularization with a new endogenous protein: rhEDI-8t. *Graefes Arch Clin Exp Ophthalmol* **250**: 731–739.
30. Ge, W, Cao, DD, Wang, HM, Jie, FF, Zheng, YF and Chen, Y (2011). Endostar combined with chemotherapy versus chemotherapy alone for advanced NSCLCs: a meta-analysis. *Asian Pac J Cancer Prev* **12**: 2901–2907.
31. Dhanabal, M, Volk, R, Ramchandran, R, Simons, M and Sukhatme, VP (1999). Cloning, expression, and *in vitro* activity of human endostatin. *Biochem Biophys Res Commun* **258**: 345–352.
32. Hanai, J, Dhanabal, M, Karumanchi, SA, Albanese, C, Waterman, M, Chan, B et al. (2002). Endostatin causes G1 arrest of endothelial cells through inhibition of cyclin D1. *J Biol Chem* **277**: 16464–16469.
33. Kim, YM, Hwang, S, Kim, YM, Pyun, BJ, Kim, TY, Lee, ST et al. (2002). Endostatin blocks vascular endothelial growth factor-mediated signaling via direct interaction with KDR/Flk-1. *J Biol Chem* **277**: 27872–27879.
34. Dixelius, J, Cross, M, Matsumoto, T, Sasaki, T, Timpl, R and Claesson-Welsh, L (2002). Endostatin regulates endothelial cell adhesion and cytoskeletal organization. *Cancer Res* **62**: 1944–1947.
35. Kim, YM, Jang, JW, Lee, OH, Yeon, J, Choi, EY, Kim, KW et al. (2000). Endostatin inhibits endothelial and tumor cellular invasion by blocking the activation and catalytic activity of matrix metalloproteinase. *Cancer Res* **60**: 5410–5413.
36. Chaves, KC, Peron, JP, Chammas, R, Turaça, LT, Pesquero, JB, Braga, MS et al. (2012). Endostatin gene therapy stimulates upregulation of ICAM-1 and VCAM-1 in a metastatic renal cell carcinoma model. *Cancer Gene Ther* **19**: 558–565.
37. Colorado, PC, Torre, A, Kamphaus, G, Maeshima, Y, Hopfer, H, Takahashi, K et al. (2000). Anti-angiogenic cues from vascular basement membrane collagen. *Cancer Res* **60**: 2520–2526.
38. Tandle, A, Blazer, DG 3rd and Libutti, SK (2004). Antiangiogenic gene therapy of cancer: recent developments. *J Transl Med* **2**: 22.
39. Marconcini, L, Marchio, S, Morbidelli, L, Cartocci, E, Albini, A, Ziche, M et al. (1999). c-fos-induced growth factor/vascular endothelial growth factor D induces angiogenesis *in vivo* and *in vitro*. *Proc Natl Acad Sci USA* **96**: 9671–9676.
40. Hübscher, SG and Strain, AJ (2005). Another Notch to be added to the list of hepatocellular growth regulatory factors? *Hepatology* **41**: 439–442.
41. Houde, C, Li, Y, Song, L, Barton, K, Zhang, Q, Godwin, J et al. (2004). Overexpression of the NOTCH ligand JAG2 in malignant plasma cells from multiple myeloma patients and cell lines. *Blood* **104**: 3697–3704.
42. Chien, MH, Ku, CC, Johansson, G, Chen, MW, Hsiao, M, Su, JL et al. (2009). Vascular endothelial growth factor-C (VEGF-C) promotes angiogenesis by induction of COX-2 in leukemic cells via the VEGF-R3/JNK/AP-1 pathway. *Carcinogenesis* **30**: 2005–2013.
43. O'Neil, JD, Owen, TJ, Wood, VH, Date, KL, Valentine, R, Chukwuma, MB et al. (2008). Epstein-Barr virus-encoded EBNA1 modulates the AP-1 transcription factor pathway in nasopharyngeal carcinoma cells and enhances angiogenesis in vitro. *J Gen Virol* **89**(Pt 11): 2833–2842.
44. Singh, NK, Van Quyen, D, Kundumani-Sridharan, V, Brooks, PC and Rao, GN (2010). AP-1 (Fra-1/c-Jun)-mediated induction of expression of matrix metalloproteinase-2 is required for 15(S)-hydroxyeicosatetraenoic acid-induced angiogenesis. *J Biological Chem* **285**: 16830–16843.
45. Beverly, A, Teicher, WML and Helman, LJ (2012). Targeting cancer metabolism. *Clin Cancer Res* **18**: 5537–5545.
46. Beale, EG, Harvey, BJ and Forest, C (2007). PCK1 and PCK2 as candidate diabetes and obesity genes. *Cell Biochem Biophys* **48**: 89–95.
47. Millward, CA, Desantis, D, Hsieh, CW, Heaney, JD, Pisano, S, Olswang, Y et al. (2010). Phosphoenolpyruvate carboxykinase (Pck1) helps regulate the triglyceride/fatty acid cycle and development of insulin resistance in mice. *J Lipid Res* **51**: 1452–1463.
48. Granneman, JG, Moore, HP, Mottillo, EP and Zhu, Z (2009). Functional interactions between Mldp (LSDP5) and Abhd5 in the control of intracellular lipid accumulation. *J Biol Chem* **284**: 3049–3057.
49. Kwong, JM, Quan, A, Kyung, H, Piri, N and Caprioli, J (2011). Quantitative analysis of retinal ganglion cell survival with Rbpms immunolabeling in animal models of optic neuropathies. *Invest Ophthalmol Vis Sci* **52**: 9694–9702.
50. Shen, Z, Yang, ZF, Gao, Y, Li, JC, Chen, HX, Liu, CC et al. (2008). The kringle 1 domain of hepatocyte growth factor has antiangiogenic and antitumor cell effects on hepatocellular carcinoma. *Cancer Res* **68**: 404–414.
51. Lum, CT, Yang, ZF, Li, HY, Wai-Yin Sun, R, Fan, ST, Poon, RT et al. (2006). Gold(III) compound is a novel chemocytotoxic agent for hepatocellular carcinoma. *Int J Cancer* **118**: 1527–1538.
52. Antigny, F, Girardin, N and Frieden, M (2012). Transient receptor potential canonical channels are required for *in vitro* endothelial tube formation. *J Biol Chem* **287**: 5917–5927.
53. Weidner, N (1995). Current pathologic methods for measuring intratumoral microvessel density within breast carcinoma and other solid tumors. *Breast Cancer Res Treat* **36**: 169–180.
54. Tanigawa, N, Lu, C, Mitsui, T and Miura, S (1997). Quantitation of sinusoid-like vessels in hepatocellular carcinoma: its clinical and prognostic significance. *Hepatology* **26**: 1216–1223.